nature biotechnology

A genetically encoded fluorescent acetylcholine indicator for *in vitro* and *in vivo* studies

Miao Jing[1–3,16], Peng Zhang[4,16], Guangfu Wang[4,5], Jiesi Feng[1–3], Lukas Mesik[6], Jianzhi Zeng[1–3], Huoqing Jiang[1–3], Shaohua Wang[7], Jess C Looby[4,8], Nick A Guagliardo[4], Linda W Langma[9], Ju Lu[10], Yi Zuo[10], David A Talmage[7], Lorna W Role[7], Paula Q Barrett[4], Li I Zhang[6], Minmin Luo[11,12], Yan Song[3], J Julius Zhu[4,13–15] & Yulong Li[1–3]

The neurotransmitter acetylcholine (ACh) regulates a diverse array of physiological processes throughout the body. Despite its importance, cholinergic transmission in the majority of tissues and organs remains poorly understood owing primarily to the limitations of available ACh-monitoring techniques. We developed a family of ACh sensors (GACh) based on G-protein-coupled receptors that has the sensitivity, specificity, signal-to-noise ratio, kinetics and photostability suitable for monitoring ACh signals *in vitro* and *in vivo*. GACh sensors were validated with transfection, viral and/or transgenic expression in a dozen types of neuronal and non-neuronal cells prepared from multiple animal species. In all preparations, GACh sensors selectively responded to exogenous and/or endogenous ACh with robust fluorescence signals that were captured by epifluorescence, confocal, and/or two-photon microscopy. Moreover, analysis of endogenous ACh release revealed firing-pattern-dependent release and restricted volume transmission, resolving two long-standing questions about central cholinergic transmission. Thus, GACh sensors provide a user-friendly, broadly applicable tool for monitoring cholinergic transmission underlying diverse biological processes.

Acetylcholine (ACh), the first identified neurotransmitter, mediates cell-to-cell communication in the central and peripheral nervous systems, as well as non-neuronal systems[1–7]. Cholinergic projection neurons within the mammalian brain originate primarily in three major nuclei, including the basal forebrain, the brainstem pedunculopontine, and laterodorsal tegmental nuclei in the brainstem. Cholinergic neurons within these groups project widely throughout the cortical and subcortical domains, consistent with their involvement in complex brain functions, including attention, perception, associative learning, and sleep/awake balancing[1–5]. Additional smaller populations of cholinergic neurons scatter throughout other brain areas (e.g., the medial habenula (MHb) and the striatum), contributing to behaviors related to motion, motivation, and stress[1,3,8]. Dysregulation of central cholinergic transmission is linked to a number of brain disorders, including Alzheimer's disease, addiction, epilepsy, Parkinson's disease, schizophrenia, and depression[9,10]. In the peripheral nervous and non-nervous systems, ACh is released by both neurons and non-neuronal cells to relay fast transmission at neuromuscular junctions and to regulate functions of a variety of other tissues and organs, including the heart, liver, and pancreas[5–7]. Dysregulation of peripheral and non-neuronal cholinergic signals is associated with multiple pathological states, including cardiovascular disease, diabetes, immune deficiency, and cancer[11,12].

Despite the significance of ACh signals in many fundamental aspects of our physiology, cholinergic transmission in the majority of tissues and organs remains poorly understood, due primarily to the limitations of tools available for the direct measurement of ACh[1,5,13]. Microdialysis, an established method for monitoring extracellular ACh[14], is less frequently used because of its poor spatial and temporal resolution. Patch-clamp recordings have excellent sensitivity and temporal resolution, but the approach is limited by the number of cells that can be recorded simultaneously and the prominent desensitization of cholinergic currents[3]. Similarly, ACh amperometry has millisecond temporal resolution, yet its technically challenging enzymatic coating procedure limits its stability and reproducibility[15]. While the TANGO assay has unparalleled sensitivity, the time-consuming transcriptional and translational amplification processes prevent its use for real-time ACh measurements[16]. Recently developed FRET sensors and cell-based fluorescent sensors (CNiFERs) for ACh have attractive real-time imaging features, but they are limited by either the low sensitivity[17,18] or the dependence on invasive cell transplantation[19,20]. These fluorescent

[1]State Key Laboratory of Membrane Biology, Peking University School of Life Sciences, Beijing, China. [2]PKU-IDG/McGovern Institute for Brain Research, Beijing, China. [3]Peking-Tsinghua Center for Life Sciences, Beijing, China. [4]Department of Pharmacology, University of Virginia School of Medicine, Charlottesville, Virginia, USA. [5]Center for Life Sciences, School of Life Science and Technology, Harbin Institute of Technology, Harbin, China. [6]Zilkha Neurogenetic Institute, Department of Physiology & Neuroscience, Keck School of Medicine, University of Southern California, Los Angeles, California, USA. [7]Department of Neurobiology and Behavior, Stony Brook University, Stony Brook, New York, USA. [8]Undergraduate Class of 2019, University of Virginia College of Arts and Sciences, Charlottesville, Virginia, USA. [9]Department of Surgery, University of Virginia School of Medicine, Charlottesville, Virginia, USA. [10]Department of Molecular, Cell, and Developmental Biology, University of California, Santa Cruz, California, USA. [11]School of Life Sciences, Tsinghua University, Beijing, China. [12]National Institute of Biological Sciences, Beijing, China. [13]School of Medicine, Ningbo University, Ningbo, China. [14]Donders Institute for Brain, Cognition and Behavior, Radboud University Nijmegen, Nijmegen, the Netherlands. [15]Department of Physiology, School of Basic Medicine, Tongji Medical College, Huazhong University of Science and Technology, Wuhan, China. [16]These authors contributed equally to this work. Correspondence should be addressed to J.J.Z. (jjzhu@virginia.edu) or Y.L. (yulongli@pku.edu.cn).

Received 5 May 2017; accepted 30 April 2018; published online 9 July 2018; doi:10.1038/nbt.4184

sensors, nevertheless, inspired us to engineer more user-friendly and broadly applicable genetically encoded ACh sensors[19,21].

Here, we report a family of genetically encoded G-protein-coupled receptor activation-based sensors for ACh (GACh). Our GACh sensors were initially constructed by coupling a circular permutated green fluorescent protein (cpGFP) into a muscarinic acetylcholine receptor (MR), with subsequent improvements via large-scale, site-directed mutagenesis and screening. The sensitivity and utility of GACh sensors were validated in cultured HEK293T cells, in cultured cortical neurons, in tissue slices prepared from multiple brain regions and peripheral organs, in the olfactory system of living *Drosophila*, and in the visual cortex of freely behaving mice *in vivo*. Our data indicate that GACh sensors have the sensitivity (EC_{50} ~1 μM), specificity (comparable to endogenous MRs), signal-to-noise ratio (SNR ~14), kinetics ($T_{on/off}$ ~200–800 ms) and photostability (~1–4 h) suitable for precise and convenient real-time assays of ACh signals.

RESULTS

Development and optimization of GACh sensors

We first inserted a conformationally sensitive cpGFP into the third intracellular loop (ICL_3) of five subtypes of human muscarinic acetylcholine receptors (M_{1-5}Rs) (Fig. 1a and Supplementary Fig. 1). ICL_3 was chosen because it links the transmembrane helices 5 and 6 of MRs and may undergo a large conformational change upon ACh binding[22]. We replaced ICL_3 of M_{1-5}Rs with a shorter 54-amino acid ICL_3 modified from the structurally well-characterized β2 adrenergic receptor (β2AR)[23] to avoid creating a lengthy cpGFP-containing ICL_3 that may hinder the expression and trafficking of the proteins (Supplementary Fig. 1b). Cells expressing the M_3R chimera showed excellent membrane expression in HEK293T cells and increased fluorescence responses ($\Delta F/F_0$) (by ~30%) to bath application of ACh (Fig. 1b and Supplementary Fig. 1a). In contrast, cells expressing the other four MR chimeras all exhibited poor membrane expression and no detectable $\Delta F/F_0$ upon ACh application (Supplementary Fig. 1b–d).

To improve this new ACh sensor (named GACh1.0), we used site-directed mutagenesis to create a library of 723 randomized point mutations at the N terminus two-amino acid and C terminus five-amino acid linkers that connect cpGFP and M_3R (Fig. 1c and Supplementary Fig. 2). When expressed in HEK293T cells, we found variants with one or multiple single-point mutations on the seven linker residues (total 18 hits) produced relatively larger $\Delta F/F_0$ responses, with the best variant (named GACh1.5) producing a ~70% increase in $\Delta F/F_0$ (Fig. 1c,d and Supplementary Fig. 2). In a second round of site-directed mutagenesis and screening, we used combinations of single top hits on N terminus linker residues (i.e., GG) and two to four top hits on C terminus linker residues, and found one variant (named GACh2.0) out of 23 combinatorial variants with the best $\Delta F/F_0$ (Fig. 1c and Supplementary Fig. 2). GACh2.0 had the same expression and membrane trafficking properties and enhanced dynamic range (by 2.5-fold) compared to GACh1.0 (Fig. 1e–g and Supplementary Movie 1), and ~20-fold larger peak signal responses and ~60-fold higher signal-to-noise ratio (SNR) compared to M_1R-based FRET sensor[18] (Fig. 1h–j and Supplementary Fig. 3).

Characterization of GACh sensors in cultured cells

Next, we measured the response kinetics of GACh2.0 (Fig. 2a,b). High-speed imaging showed that rapid local perfusion of agonist ACh or antagonist tiotropium (Tio) elicited increases or decreases in fluorescence intensity of GACh2.0, with average activation (on) and inactivation (off) time constants of 280 ± 32 ms and 762 ± 75 ms, respectively (Fig. 2b,c). These values were likely overestimated due to the slow drug application/perfusion system (~80 ms delay, Supplementary Fig. 4). Moreover, confocal imaging indicated that GACh sensors had a photostability comparable to or better than GCaMP6s and EGFP (Supplementary Fig. 5). Altering extracellular pH with buffers (pH 5–9) resulted in modest fluorescence changes in GACh-expressing cells (Supplementary Fig. 6a,b), suggesting a weak pH dependency. In the permeabilized condition, the fluorescence of GACh sensors exhibited larger pH dependency with a pK_a close to 7 (Supplementary Fig. 6c,d).

To measure the sensitivity of GACh2.0, we progressively increased ACh from 10 nM to 100 μM, which increased the fluorescence intensity in GACh2.0-expressing cells, yielding an EC_{50} (concentration for 50% maximal effect) of ~0.7 μM (Fig. 2d,e), a value comparable to wild-type M_3Rs[24]. ACh-induced fluorescence signals were completely blocked by co-application of 20 μM AF-DX 384, another muscarinic antagonist[25], indicating specific responses. We also characterized the downstream signaling of GACh sensors. GACh2.0-expressing cells exhibited less receptor internalization in the presence of ACh, as well as reduced TANGO assay signal (β-arrestin-dependent) compared to wild-type M_3Rs-expressing cells (Supplementary Fig. 7a,b). Moreover, the coupling efficiency from GACh2.0 to the Gq-dependent calcium signaling was about sevenfold smaller compared to wild-type M_3Rs (Supplementary Fig. 7c–e), and there was no detectable coupling of GACh2.0 to the Gs-dependent signaling pathway (Supplementary Fig. 7f–h).

We next verified several properties of GACh sensors in cultured rat cortical neurons (Fig. 2f–j). Approximately 48 h after transfection, GACh1.0 and GACh2.0 were expressed throughout the neuronal membrane, with the majority of sensors delivered to the neurites (Fig. 2f). ACh enhanced the fluorescence intensity of GACh1.0 and GACh2.0 by ~30% and ~90%, respectively (Fig. 2g and Supplementary Movie 2), validating their functionality in neurons. Varying ACh concentration in the bath solution from 10 nM to 100 μM progressively increased the fluorescence intensity in GACh2.0-expressing neurons, with an EC_{50} of ~2 μM (Fig. 2h). In contrast, bath application of nicotine, choline, glycine, serotonin (5-HT), epinephrine, GABA, glutamate, dopamine, norepinephrine, histamine, and adenosine did not induce any detectable fluorescence responses. Moreover, ACh-induced fluorescence responses were blocked by bath-applied Tio (Fig. 2i,j). Finally, we noted no alteration in membrane fluorescence intensity in GACh2.0-expressing neurons during a 30-min bath application of 100 μM ACh (Supplementary Fig. 8a–c), consistent with the minimal arrestin-dependent internalization (Supplementary Fig. 7a,b).

Validation of GACh sensors in cultured brain slices

To generalize the applicability of GACh sensors, we expressed them in CA1 pyramidal neurons in cultured mouse hippocampal slices. Two-photon imaging showed that GACh1.0, GACh1.5, and GACh2.0 were expressed throughout CA1 pyramidal neurons by the lentiviral system, with evident fluorescence signals at the plasma membrane of somata, dendrites, and spines, sites of excitatory synapses (Supplementary Fig. 9). Next, we chose the Sindbis viral expression system that permitted a more rapid (~18 h) and robust expression of GACh sensors (Supplementary Figs. 10a and 11a). Fluorescence responses captured by an epifluorescence microscope showed that a brief 500-ms puff application of ACh or the muscarinic agonist oxotremorine[24] evoked fluorescence responses in CA1 neurons expressing GACh1.0, GACh1.5, or GACh2.0, whereas puff application of a nicotinic receptor agonist, nicotine, or control bath solution ACSF induced no responses in same neurons (Supplementary Figs. 10b–d and 11b and Supplementary Movies 3 and 4).

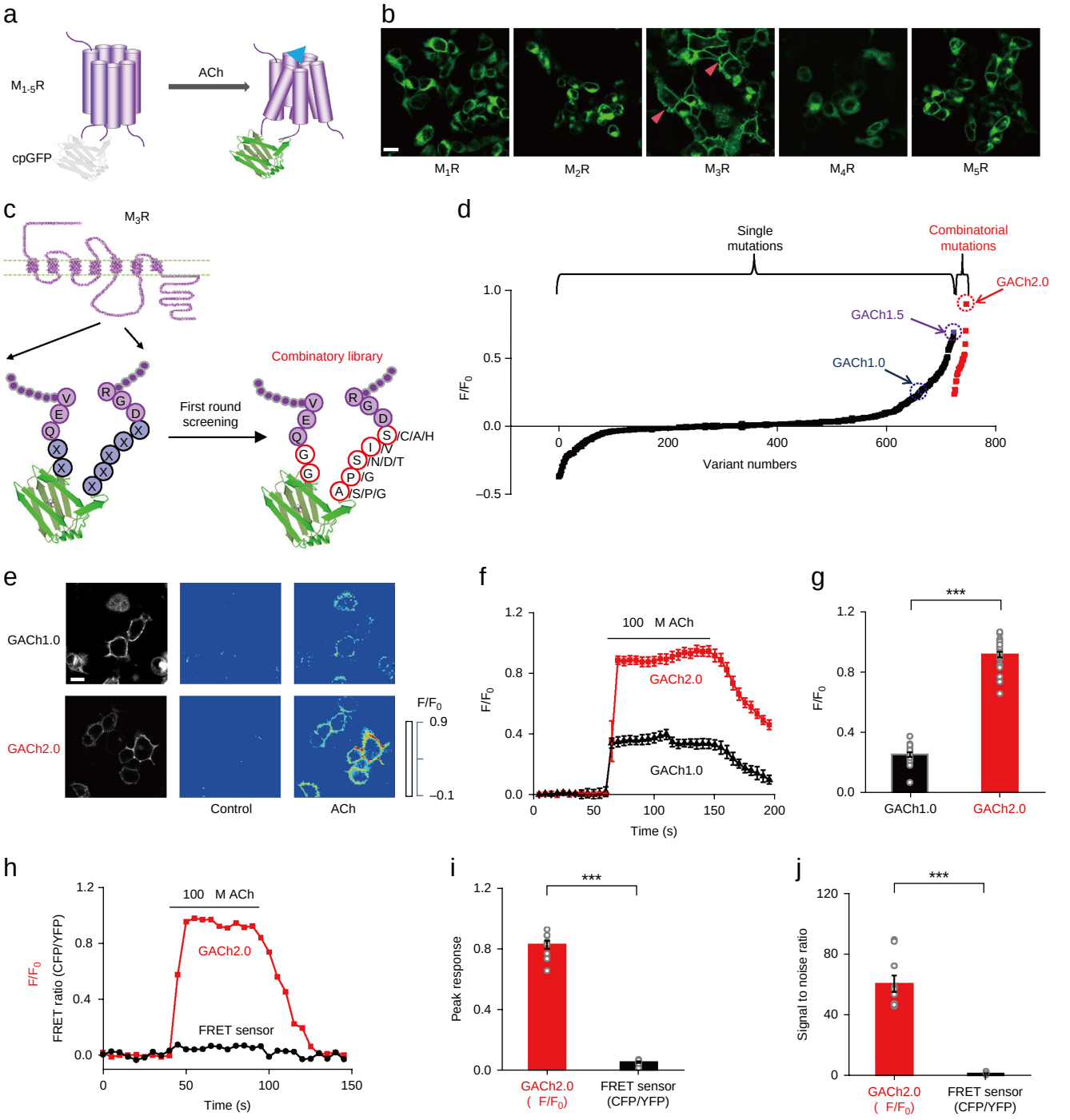

Figure 1 Development of GACh sensors. (**a**) Schematic drawing shows the principle of the GACh sensor. (**b**) Membrane expression of the different MR-based candidate GACh sensors in HEK293T cells. The red arrow heads indicate membrane-localized signals. (**c**) Schematic drawing illustrates variants with one or multiple single-point mutations on the seven linker residues (total 18 hits). (**d**) Fluorescence responses of HEK293T cells expressing one of ~750 candidate GACh sensors harboring either randomized point or combinatorial mutations to the bath application of 100 M ACh. Note F/F_0 of the combinatorial mutation-harboring GACh2.0 to be ~100% and data points are averaged responses of 2–10 cells. (**e**) Fluorescence responses of GACh1.0- and GACh2.0-expressing cells to the bath application of ACh. (**f**,**g**) F/F_0 of GACh1.0- and GACh2.0-expressing cells to ACh application (GACh1.0: 24.6 o1.5%, n = 19 cells from five cultures, GACh2.0: 90.1 o1.7%, n = 29 cells from eight cultures, U = 551, P = 6.72 × 10^{-9}). (**h**) Fluorescence responses of HEK293T cells expressing either GACh2.0 or M_1R-based FRET sensor to the application of ACh (100 M). (**i**,**j**) Averaged F/F_0 or $FRET ratio (GACh2.0: 94.0 o3.0%, n = 10 cells from two cultures; FRET: 6.61 o0.4%, n = 10 cells from two cultures, U = 100, P = 1.09 × 10^{-5}) and SNR (GACh2.0: 60.0 o5.4, n = 10 cells from two cultures; FRET: 1.12 o0.21, n = 10 cells from two cultures, U = 100, P = 1.83 × 10^{-4}) of GACh2.0 and M_1R-based FRET-sensor-expressing cells to ACh application. Data are shown as mean os.e.m., with error bars indicating s.e.m. Experiments in **b** and **e** were repeated independently for more than five cultures with similar results. ***P < 0.001 (Mann–Whitney Rank Sum non-parametric tests, two-sided). All scale bars, 10 m.

Focusing on GACh2.0, which produces the largest $\Delta F/F_0$, we found that repetitive puffs induced the same fluorescence responses in GACh2.0-expressing CA1 neurons (Supplementary Fig. 12, indicating robust photostability. As a control, bath application of 1 μM atropine, a muscarinic antagonist[25], but not 2,2,6,6-tetramethylpiperidin-4-yl heptanoate (TMPH), a nicotinic antagonist[26], completely

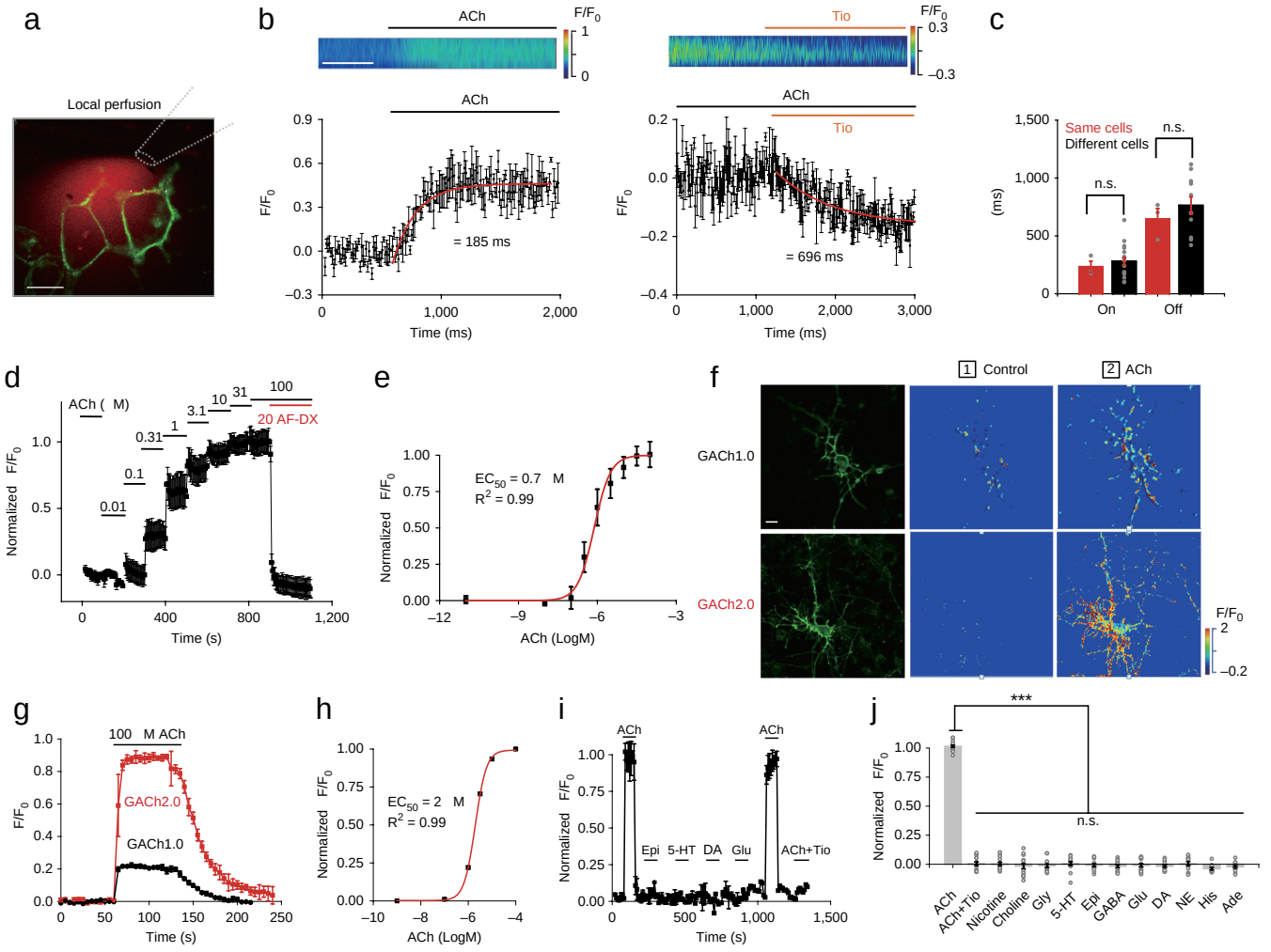

Figure 2 Characterization of GACh sensors in cultured HEK293T cells and neurons. (**a**) Illustration of a fast perfusion system with a glass pipette filled with ACh and red Rhodamine-6G dye placed close to a GACh2.0-expressing cell. The red dashed line indicates where the line scanning was performed. (**b**) Upper, scanning traces of fluorescence responses of GACh2.0-expressing cells to application of ACh and Tio. Lower, plot shows fluorescence values of on and off responses of a GACh2.0-expressing cell to the application of ACh or Tio, averaged from three different ROIs on the scanning line. The original data were processed with 16× binning and plotted. The white line indicates 0.5 s. (**c**) Averaged on and off time constants measured from the same (on: 233 ± 48 ms, n = 3 cells from three cultures; off: 645 ± 90 ms, n = 3 cells from three cultures) and different (on: 279 ± 32 ms, n = 18 cells from 18 cultures; off: 762 ± 75 ms, n = 11 cells from 11 cultures) cells. n.s., not significant. P = 0.80 for on kinetics; P = 0.64 for off kinetics. (**d**) Averaged responses (three trials from the same cell) of a GACh2.0-expressing HEK293T cell to ACh application. Note blockade of the responses by muscarinic antagonist AF-DX 384. (**e**) Dose-dependent response plot of GACh2.0-expressing HEK293T cells to ACh application yielded $pEC_{50} = -6.12 \pm 0.11$ M, or $EC_{50} = 0.78 \pm 0.25$ μM, n = 4 cells from four cultures. (**f**) Confocal GFP fluorescent and pseudocolor images of GACh1.0- and GACh2.0-expressing cultured cortical neurons in the normal bath solution and solution containing 100 μM ACh. (**g**) Time course of the fluorescence response of GACh1.0- and GACh2.0-expressing cultured neurons (averaged from three independent trials of single neurons). (**h**) Dose-dependent responses of GACh2.0-expressing cultured neurons ($pEC_{50} = -5.70 \pm 0.01$ M or $EC_{50} = 1.99 \pm 0.05$ μM; n = 15 neurons from 15 cultures). (**i**) Responses of GACh2.0-expressing neurons to application of ACh and ACh-related compounds and other major neurotransmitters/modulators (averaged from three neurons in the same culture). (**j**) Values for normalized $\Delta F/F_0$ of GACh2.0-expressing cells to application of 100 μM ACh with 2 μM tiotropium (Tio), 50 μM nicotine, 100 μM choline, 10 μM glycine (Gly), 1 μM 5-HT, 10 μM epinephrine (Epi), 10 μM GABA, 10 μM glutamate (Glu), 20 μM dopamine (DA), 200 μM norepinephrine (NE), 1,000 μM histamine (His), 1 μM adenosine (Ade) compared to application of ACh alone (ACh: 100.65 ± 7.61%, n = 14 ROIs with >10 cells each ROI; ACh+Tio: 0.19 ± 1.53%, n = 14 ROIs, U = 196, $P = 7.47 \times 10^{-6}$; nicotine: 0.32 ± 1.47%, n = 15 ROIs, U = 210, $P = 5.10 \times 10^{-6}$; choline: –1.46 ± 2.31%, n = 15 ROIs, U = 210, $P = 5.10 \times 10^{-6}$; glycine: –1.36 ± 1.58%, n = 13 ROIs, U = 182, $P = 1.13 \times 10^{-5}$; 5-HT: 0.96 ± 1.11%, n = 15 ROIs, U = 210, $P = 5.10 \times 10^{-6}$; Epi: –0.77 ± 1.35%, n = 14 ROIs, U = 196, $P = 7.47 \times 10^{-6}$; GABA: –2.01 ± 1.11%, n = 15 ROIs, U = 210, $P = 5.10 \times 10^{-6}$; Glu: –0.49 ± 1.45%, n = 16 ROIs, U = 224, $P = 3.57 \times 10^{-6}$; DA: –0.83 ± 1.20%, n = 15 ROIs, U = 210, $P = 5.10 \times 10^{-6}$; NE: –0.42 ± 1.63%, n = 12 ROIs, U = 168, $P = 1.75 \times 10^{-5}$; His: –4.54 ± 0.66%, n = 11 ROIs, U = 154, $P = 2.81 \times 10^{-5}$; Ade: –2.23 ± 1.05%, n = 16 ROIs, U = 224, $P = 3.57 \times 10^{-6}$. Data are shown as mean ± s.e.m. with error bars indicating s.e.m. *P < 0.05; **P < 0.01; ***P < 0.001; n.s., not significant (Mann–Whitney Rank Sum non-parametric tests, two-sided). All scale bars, 10 μm.

blocked ACh-induced fluorescence responses in GACh2.0-expressing neurons (Supplementary Fig. 12). Simultaneous patch-clamp recordings showed that the resting membrane potential, input resistance, membrane time constant and average spiking frequency of GACh2.0-expressing CA1 neurons were not different from nearby control non-expressing neurons (Supplementary Fig. 13a–d), suggesting GACh2.0 expression had no effect on basic membrane properties. Moreover, AMPA, NMDA, and GABAergic responses, as well as paired pulse facilitation of AMPA responses in GACh2.0-expressing neurons, remained unchanged (Supplementary Fig. 13e–h), indicating GACh2.0 expression did not alter synaptic transmission. Collectively, these results are consistent with the finding that GACh2.0 is a selective, photostable ACh sensor with minimal perturbation on cellular physiology.

To compare GACh2.0 imaging with patch-clamp recordings, we simultaneously made whole-cell recordings and fluorescence imaging from pairs of neighboring GACh2.0-expressing and non-expressing CA3 pyramidal neurons, which performed robust current response to cholinergic stimulation in cultured mouse hippocampal slices[27] (Fig. 3a). A 500-ms ACh puff evoked a brief, large inward current followed by a prolonged, small inward current in both GACh2.0-expressing and non-expressing neurons, presumably representing activation of endogenous nicotinic and muscarinic receptors, respectively[3] (Fig. 3b,d). A concurrent fluorescence signal was observed only in GACh2.0-expressing neurons, but not in control non-expressing CA3 neurons (Fig. 3b,c). The latencies of cholinergic currents and fluorescence responses were the same in GACh2.0-expressing neurons (Fig. 3b,e), indicating that GACh2.0 detected ACh as fast as endogenous cholinergic receptors. SNR of GACh2.0 fluorescence responses (~14) seemed to be smaller than that of the fast nicotinic-like cholinergic currents (~35), but larger than that of the slow muscarinic-like cholinergic currents (~8) (Fig. 3b,f), indicating a relatively comparable sensitivity for GACh2.0 to electrophysiological recording in monitoring cholinergic signals. The second ACh puff evoked same fluorescence responses, but smaller cholinergic currents (reduced by ~40%) in GACh2.0-expressing neurons compared to the first ACh puff (Fig. 3b,g,h), due presumably to the desensitization of endogenous receptors[3]. There was no difference in the amplitude, latency, or SNR of cholinergic currents in GACh2.0-expressing and non-expressing neurons (Fig. 3b–f), further confirming that expression of GACh2.0 had little non-specific effect on CA3 neurons.

GACh sensors in acute brain slices

We next imaged the fluorescence response of GACh2.0 in acute slices of distinct neuronal preparations, including layer 2 (L2) stellate neurons and L1 interneurons in the medial entorhinal cortex (MEC), L5 pyramidal neurons in the barrel cortex of mice, GABAergic thalamic reticular neurons, and glutamatergic thalamocortical neurons in the ventral basal nucleus of rats. Approximately 18 h after *in vivo* Sindbis viral expression and acute slice preparation, we measured $\Delta F/F_0$ responses to a brief puff application of ACh (Supplementary Fig. 14a). ACh and oxotremorine, but not nicotine or control bath solution ACSF, evoked robust fluorescence increases in GACh2.0-expressing neurons in all the preparations (Supplementary Fig. 14).

To further test whether GACh2.0 can report endogenously released ACh, we measured $\Delta F/F_0$ responses of GACh2.0-expressing entorhinal L2 stellate neurons to electrical stimulation of MEC L1 (Fig. 4a), a layer that is densely innervated by cholinergic fibers originating from the basal forebrain[28,29]. In GACh2.0-expressing neurons, 20 pulses at 2-Hz evoked robust fluorescence responses in GACh2.0-expressing neurons (Fig. 4b and Supplementary Movie 5), and repeated electrical stimuli delivered every 8 min induced the same $\Delta F/F_0$ responses in GACh2.0-expressing neurons (Fig. 4c,d), indicating the suitability of GACh2.0 in monitoring ACh signals over long periods. Systematically varying the stimulation frequency revealed that low-frequency stimuli (0.5–2 Hz) evoked large, plateau-like fluorescence responses, intermediate-frequency stimuli (4–12 Hz) elicited more rapidly rising but briefer fluorescence responses, while high-frequency stimuli ($\geq$20 Hz) induced minor fluorescence responses (Fig. 4e–g). Given that basal forebrain cholinergic neurons in behaving animals prefer low frequency (~0.5–2 Hz) tonic firing and theta rhythmic (~4–12 Hz) phasic firing[30,31], these results suggest that these two preferred firing patterns generate distinct sustained or transient ACh release. Further altering the number of electrical pulses delivered at 2 Hz showed that single pulses elicited detectable $\Delta F/F_0$ responses, whereas multiple pulses induced enhanced $\Delta F/F_0$ responses (Fig. 4h–j), suggesting the possible scaling of amount of released ACh by the number of presynaptic action potentials. Of note, adding 20 μM (5*R*,6*R*)6-(3-propylthio-1,2,5-thiadiazol-4-yl)-1-azabicyclooctane (PTAC), an antagonist of $M_{1,3,5}$Rs[32], to the bath solution blocked the electrically evoked $\Delta F/F_0$ responses (Supplementary Fig. 15), indicating the detection of cholinergic signals.

We noted that at times, the minimal electrical-stimulation-evoked fluorescence responses exhibited obvious spatial heterogeneity across subcellular regions of GACh2.0-expressing L2 stellate neurons. Analysis of the evoked fluorescence responses revealed one or a few subcellular hot spots, or regions of interest (ROIs), with the largest $\Delta F/F_0$ responses, whereas other ROIs had smaller or undetectable changes in $\Delta F/F_0$ (Fig. 4l–n), suggesting the spatially restricted release and clearance of ACh. Plotting $\Delta F/F_0$ responses at all ROIs against the distance from the ROI with the largest $\Delta F/F_0$ responses yielded a volume transmission spread-length constant of 9.0 μm for MEC L2 stellate neurons (Fig. 4n). To verify this surprisingly small cholinergic volume transmission, we examined the minimal electrical-stimulation-evoked local fluorescence responses along the somatodendritic axis of GACh2.0-expressing hippocampal CA1 neurons (Supplementary Fig. 16a). Consistent with previous studies[27], we found that electrical stimuli of the stratum-oriens and pyramidale were most likely to elicit cholinergic responses in CA1 neurons (Supplementary Fig. 16b,c). The largest fluorescence responses were typically observed at one or a few subcellular ROIs in the soma of GACh2.0-expressing neurons, whereas fluorescence responses at other ROIs in the soma and dendrite of the same neurons were much smaller or undetectable (Supplementary Fig. 16b,c). Similar analysis gave a volume transmission spread-length constant of 15.6 μm for CA1 neurons (Supplementary Fig. 16d). Bath application of ACh, as a control, induced similar $\Delta F/F_0$ responses along the somatodendritic axis of GACh2.0-expressing CA1 neurons (Supplementary Fig. 16e), ruling out the non-specific effect of unequal expression.

To determine whether GACh sensors may report other ACh release modes, we studied neurons in the medial habenula (MHb), which potentially release ACh during high-frequency firing[8,33]. GACh2.0 sensors were successfully expressed in interpeduncular nucleus (IPN) by adeno-associated virus (AAV), and in close proximity with MHb cholinergic fibers, verified by post hoc ChAT immunostaining (Supplementary Fig. 17a–c). Two-photon imaging of GACh2.0-expressing neurons showed that brief 1-, 10-, 20-, or 50-Hz 5-s electrical stimuli evoked no detectable fluorescence changes, whereas 100-Hz stimuli elicited small $\Delta F/F_0$ responses (Supplementary Fig. 17d,e). Bath application of GABA or $GABA_B$ receptor agonist baclofen enhanced $\Delta F/F_0$ responses in a frequency-dependent manner, consistent with our

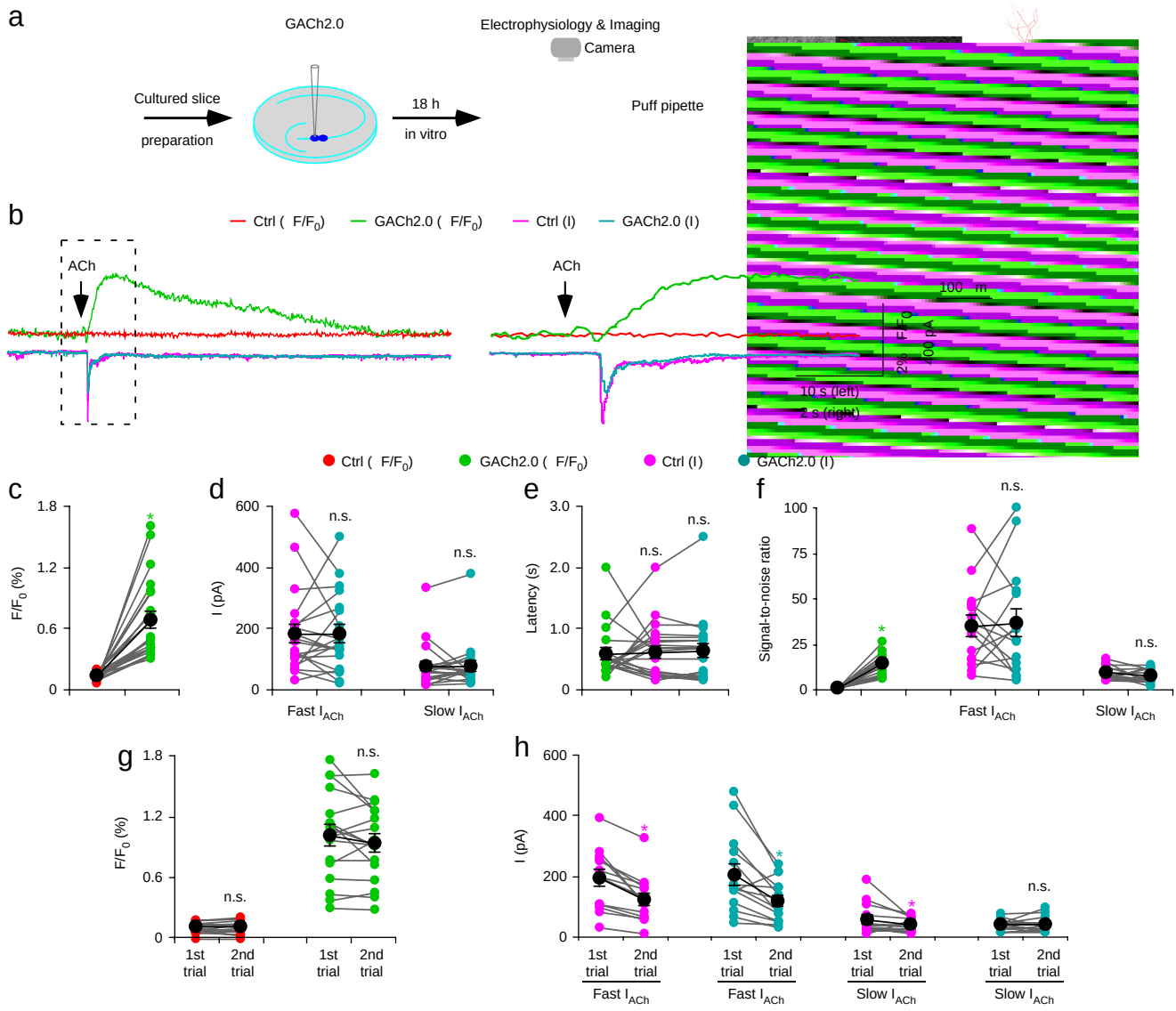

Figure 3 GACh2.0 detects rapid ACh application in brain slices. (**a**) Schematic drawing of the design of simultaneous imaging and electrophysiological recording experiments in mouse cultured hippocampal slice preparation. Left insets show transmitted light (top), fluorescence microscopic (bottom) images of a pair of simultaneously recorded GACh2.0-expressing and neighboring control non-expressing CA3 neurons. Right insets show the biocytin-filled and reconstructed GACh2.0-expressing and non-expressing CA3 neurons. (**b**) Left, simultaneous fluorescence and current responses of the pair of GACh2.0-expressing and neighboring control non-expressing CA3 neurons to a brief puff (500 ms) application of 100 mM acetylcholine (ACh). Right, the responses in the left rectangle box are shown again on an expanded time scale. (**c**) Values for the cholinergic fluorescence responses of GACh2.0-expressing CA3 neurons compared to non-expressing neurons (GACh2.0: 0.68 ±0.08%; Ctrl: 0.14 ±0.01%; Z = 4.015; P = 0.0005; n = 21 neurons from nine animals). (**d**) Values for the amplitudes of fast cholinergic current responses (GACh2.0: 180.9 ±30.8 pA; Ctrl: 181.2 ±28.4 pA; Z = –0.037; P = 0.97; n = 21 from nine animals) and slow cholinergic current responses (GACh2.0: 76.2 ±15.9 pA; Ctrl: 76.8 ±17.0 pA; Z = 0.896; P = 0.37; n = 21 neurons from nine animals) in GACh2.0-expressing CA3 neurons compared to non-expressing neurons. (**e**) Values for the latencies of cholinergic current responses in non-expressing CA3 neurons (Ctrl: 611 ±10 ms; Z = 0.523; P = 0.60) and GACh2.0-expressing (GACh2.0: 622 ±12 ms; Z = 0.485; P = 0.62) compared to those of fluorescence responses of GACh2.0-expressing neurons (GACh2.0: 580 ±9 ms; n = 21 neurons from nine animals). (**f**) Values for the signal-to-noise ratio of cholinergic fluorescence responses of GACh2.0-expressing compared to non-expressing CA3 neurons (GACh2.0: 14.0 ±1.5; Ctrl: 1.0 ±0.1; Z = 3.408; P = 0.001; n = 15 neurons from six animals), and that of fast (GACh2.0: 36.2 ±7.7; Ctrl: 34.6 ±5.7; Z = 0.170; P = 0.86; n = 15 neurons from six animals) and slow (GACh2.0: 7.5 ±1.0; Ctrl: 9.0 ±1.0; Z = -0.852; P = 0.39; n = 15 neurons from six animals) cholinergic current responses of GACh2.0-expressing compared to non-expressing CA3 neurons. Note that SNR of cholinergic fluorescence responses of GACh2.0-expressing CA3 neurons is smaller than fast (GACh2.0: Z = 2.242; P = 0.015; Ctrl: Z = 3.124; P = 0.002), but larger than slow (GACh2.0: Z = –2.840; P = 0.005; Ctrl: Z = –2.669; P = 0.008) cholinergic current responses of GACh2.0-expressing compared to non-expressing CA3 neurons. I, the cholinergic current recorded. (**g**) Values for the two fluorescence responses of non-expressing (1st: 0.11 ±0.01%; 2nd: 0.11 ±0.01%; Z = -0.142; P = 0.89; n = 17 neurons from nine animals) and GACh2.0-expressing (1st: 1.01 ±0.11%; 2nd: 0.94 ±0.09%; Z = –1.138; P = 0.26; n = 17 neurons from nine animals) CA3 neurons. (**h**) Values for the two fast cholinergic current responses in non-expressing (1st: 190.9 ±26.1 pA; 2nd: 124.1 ±20.4 pA; Z = –3.296; P = 0.001; n = 17 neurons from nine animals) and GACh2.0-expressing (1st: 203.8 ±34.9 pA; 2nd: 119.3 ±18.6 pA; Z = –2.856; P = 0.004; n = 17 neurons from nine animals) CA3 neurons, and values for the two slow cholinergic current responses of non-expressing (1st: 56.4 ±13.4 pA; 2nd: 39.0 ±5.7 pA; Z = –2.166; P = 0.003; n = 17 neurons from nine animals) and GACh2.0-expressing (1st: 41.6 ±4.5 pA; 2nd: 41.7 ±6.8 pA; Z = 0.940; P = 0.93; n = 17 neurons from nine animals) CA3 neurons. Data are shown as mean ±s.e.m., where large black dots indicate mean response, error bars indicate s.e.m. *P < 0.05 (Wilcoxon tests, two-sided).